THE JOURNAL OF PHYSICAL CHEMISTRY B

Article

pubs.acs.org/JPCB

Small-Angle Neutron-Scattering Studies of Mixed Micellar Structures Made of Dimeric Surfactants Having Imidazolium and Ammonium Headgroups

Asish Pal,[†,⊥] Sougata Datta,[†,⊥] V. K. Aswal,[∥] and Santanu Bhattacharya*[,†,‡,§]

[†]Department of Organic Chemistry, Indian Institute of Science, Bangalore 560012, India

[‡]Chemical Biology Unit, JNCASR, Bangalore 560 012, India

[§]J. C. Bose Fellow, Department of Science and Technology, New Delhi, India

[∥]Solid State Physics Division, Bhabha Atomic Research Centre, Mumbai 400085, India

ABSTRACT: Planar imidazolium cation based gemini surfactants [16-Im-*n*-Im-16], $2Br^-$ (where n = 2, 3, 4, 5, 6, 8, 10, and 12), exhibit different morphologies and internal packing arrangements by adopting different supramolecular assemblies in aqueous media depending on their number of spacer methylene units $(CH_2)_n$. Detailed measurements of the small-angle neutron-scattering (SANS) cross sections from different imidazolium-based surfactant micelles in aqueous media (D_2O) are reported. The SANS data, containing the information of aggregation behavior of such surfactants in the molecular level, have been analyzed on the basis of the Hayter and Penfold model for the macro ion solution to compute the interparticle structure factor $S(Q)$ taking into account the screened Coulomb interactions between the dimeric surfactant micelles. The characteristic changes in the SANS spectra of the dimeric surfactant with n = 4 due to variation of temperature have also been investigated. These data are then compared with the SANS characterization data of the corresponding gemini micelles containing tetrahedral ammonium ion based polar headgroups. The critical micellar concentration of each surfactant micelle (cmc) has been determined using pyrene as an extrinsic fluorescence probe. The variation of cmc as a function of spacer chain length has been explained in terms of conformational variation and progressive looping of the spacer into the micellar interior upon increasing the n values. Small-angle neutron-scattering (SANS) cross sections from different mixed micelles composed of surfactants with ammonium headgroups, 16-A_0, [16-Am-*n*-Am-16], $2Br^-$ (where n = 4), 16-I_0, and [16-Im-*n*-Im-16], $2Br^-$ (where n = 4), in aqueous media (D_2O) have also been analyzed. The aggregate composition matches with that predicted from the ideal mixing model.

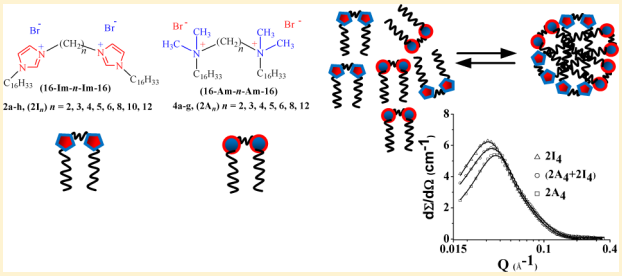

INTRODUCTION

Surfactant molecules, which contain a polar headgroup and a hydrophobic chain, are capable of producing self-organizing systems such as micelles, bilayers, lamellae, and vesicles.[1,2] The properties of such aggregates are distinctly different from those of the individual surfactant monomer prior to aggregation.[3−5] Attempts to correlate the aggregate properties with that of the molecular features of the surfactant are important for developing new surfactant systems for specific household and industrial applications.[6,7] In this context, the dimeric or gemini surfactants, consisting of two hydrophobic chains and two polar headgroups covalently attached through a spacer, are of particular interest. This is owing to their unusual properties, such as low critical micellar concentrations (cmc), better catalytic properties, higher adsorption efficiency, and enhanced abilities for lowering the oil−water interfacial tension as compared to their single-chain monomeric analogues.[8−10]

Micelles and similar self-organized assemblies have been the subject of intense research for a number of years.[11] The cationic micelles are of interest since the report of micellar growth and increasing viscoelasticity of the mixture of CTAB and sodium salicylate appeared in the literature.[12] Such additives reduce the repulsion between the cationic headgroups of the surfactants, which leads to a marked increase in the viscoelasticity with eventual formation hydrogels.[13−15] In this regard, noninvasive techniques such as small-angle neutron-scattering allow the structural elucidation of the assemblies formed by different surfactants.[11,16−20] From earlier small-angle neutron-scattering (SANS) studies[21−23] on the micelles derived from the gemini ammonium surfactants, [16-Am-*n*-Am-16], $2Br^-$ (for simple abbreviation $2A_n$), where n = 3, 4, 5, 6, 8, 10, 12, and their mixtures with cetyl trimethyl ammonium bromide (CTAB),[22] it became clear that the extent of aggregate growth and the variations of shapes of the gemini micelles and their mixed micelles with monomeric CTAB depend primarily on the nature and the length (n-values) of the spacer chain. We also

Received: May 15, 2012
Revised: August 20, 2012
Published: September 20, 2012

studied the effect of changing the nature of the spacer chain from hydrophobic polymethylene to hydrophilic oxyethylene on the micellar organizations.[23] In the process of continuing structure−property correlation of various surfactant assemblies, we reported the formation of different micellar morphology, e.g., ellipsoidal to rod and disk upon changing the polymethylene spacer for the gemini surfactant with phosphate headgroup.[24] Also, increasing the number of headgroups in a surfactant molecule resulted in a visible change in the size of the micelles, and this observation was true irrespective of ammonium or pyridinium multiheaded surfactants.[25−27]

On the other hand, ionic liquid[28,29] type molecules are molten salts that remain as liquid at room temperature, and they represent an interesting medium for various reactions.[30] Seddon and Rogers independently demonstrated that certain imidazolium and pyridinium cations in combination with several anions such as chloride, tetrafluoroborate, and hexafluorophosphate etc. are potential room-temperature ionic liquids (RTIL).[31−33] Thus, surfactants based on imidazolium headgroups are of considerable interest.[34−36] However, the structural properties of micelles derived from the imidazolium cation based surfactants have not been investigated in contrast to their ammonium ion based cationic surfactant analogues. These imidazolium-based gemini surfactants are interesting owing to the structural similarity at the molecular level with that of the ionic liquid forming system. The delocalized character of the cationic headgroup in such imidazolium surfactants endows them with superior properties such that potential applications in many areas like skin care, medicine, life science, petrochemistry, etc. have been envisaged.[37,38] Therefore, it is important to study the property of ionic liquid like gemini surfactants. Indeed, the gemini imidazolium surfactants with different hydrophobic chain lengths have been compared with their corresponding monomers recently.[39] Recently, the DNA binding affinity of thioether spacers containing imidazolium gemini surfactants has been investigated by agarose gel electrophoresis and ethidium bromide exclusion experiments.[40]

In this work, we investigated the SANS of various gemini micelles (Chart 1) to understand the role of the rigid imidazolium headgroup on the micelle forming ability. We also compared the micellar structures of this class of surfactants with that of their ammonium gemini cationic counterpart. The effect of temperature on the neutron cross sections of both classes of surfactant was examined. We have also examined the variation of neutron cross sections of the mixed micelles composed of monomeric and gemini ammonium and imidazolium surfactants. We show herein how the micellar shapes, aggregation number, and ionization, etc. change with variation in the structures of the headgroups.

Chart 1. Molecular Structures of the Various Monomeric and Gemini Surfactants Used in the Present Study

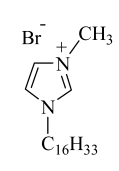

1, (16-Im), I_0

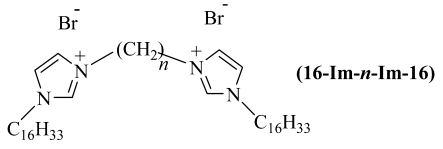

(16-Im-*n*-Im-16)

2a-h, ($2I_n$) n = 2, 3, 4, 5, 6, 8, 10, 12

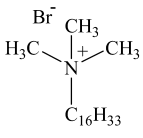

3, (16-Am), A_0

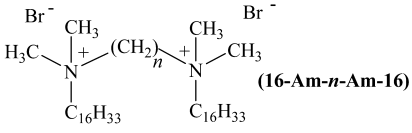

(16-Am-*n*-Am-16)

4a-g, ($2A_n$) n = 2, 3, 4, 5, 6, 8, 12

EXPERIMENTAL SECTION

Materials. All the reagents and solvents used for the present study were of the highest grade available commercially and used purified, dried, or freshly distilled as required. Imidazole, *N*-methylimidazole, *n*-hexadecyl bromide, pyrene, and α,ω-dibromo alkanes were bought from Aldrich chemical company. Each of the synthesized compounds was characterized by ^{1}H NMR spectra recorded in $CDCl_3$ in a Bruker 400 MHz NMR spectrometer. Chemical shifts (δ) are reported in parts per million downfield from the internal standard (TMS).

The imidazolium monomeric (I_o) and gemini surfactants ($2I_n$) were synthesized in this laboratory by using the method described by Dupont and co-workers.[41] Gemini ammonium surfactants ($2A_n$) were synthesized as reported earlier.[21]

Determination of Critical Micellar Concentration (CMC). A pyrene-based fluorescence method[42,43] was used for the determination of cmc values of each of these surfactants. Recrystallized pyrene was taken as the fluorescence probe whose emission intensity increased when it was incorporated into the micellar interior from the bulk aqueous medium. Fluorescence emission measurement was carried out in a Hitachi F-4500 fluorescence spectrometer connected to a thermostat water circulating bath (Julabo model F10) at 30 °C and using a 3 cm^3 cell. Excitation wavelength was chosen at 337 nm, and the emission spectrum was recorded in the range of 360−410 nm. Slit widths of 5 nm were selected for both excitation and emission. Aqueous solutions of each gemini surfactant at various concentrations were doped with a fixed concentration (0.5 μM) of pyrene for the determination of cmc values. The corresponding cmc values were obtained from the plots of concentrations of a given surfactant vs the ratio (I_3/I_1) of the intensities of the first (I_1) and third vibronic peaks due to pyrene in the emission spectra.

Small-Angle Neutron-Scattering (SANS) measurements. *Data Collection.* Small-angle neutron-scattering (SANS) experiments were carried out on [16-Am-*n*-Am-16], $2Br^-$ ($2A_n$), and [Im-*n*-Im], 2Br- ($2I_n$), samples for n = 2, 3, 4, 5, 8, and 12. All the solutions used in neutron scattering experiments were prepared in D_2O. Solution in D_2O provides a very good contrast between the micelles and the solvent in a SANS experiment. Neutron scattering measurements were performed on the 7.0 m (source-to-detector distance) SANS instrument at the Dhruva reactor, Trombay.[44] The sample-to-detector distance was maintained at 1.8 m for all runs. This spectrometer makes use of a BeO filtered beam, and the angular distribution of the scattered neutrons is recorded using a one-dimensional positron-sensitive detector (PSD). The accessible wave vector transfer, Q (= 4π sin $0.5\theta/\lambda$, where λ is the wavelength of the incident neutrons and θ is the scattering angle), range of this instrument is between 0.017 and 0.35 $Å^{-1}$. The PSD allows a simultaneous recording of the data over the full Q range. The mean wavelength (λ) was kept at 0.52 nm having delta $\Delta\lambda/\lambda$ about 15%. The sample solution was held in a 0.5 cm path length UV grade quartz sample holder with tight-fitting Teflon stoppers, sealed with parafilm. In most of the measurements, the surfactant concentration (c = 25 mM) and

dx.doi.org/10.1021/jp304700t | J. Phys. Chem. B 2012, 116, 13239−13247

the sample temperature were kept fixed. The effect of different temperatures was investigated for both the $2I_n$ and $2A_n$ micellar systems at a fixed surfactant concentration of c = 25 mM.

Data Treatment. Scattering intensities from the surfactant solutions were corrected for detector background and sensitivity, empty cell scattering, and sample transmission. The resulting corrected intensities were normalized to absolute cross-section units, and thus $d\Sigma/d\Omega$ vs Q was obtained. The experimental points are fitted using a nonlinear least-squares routine as described below. A comparison between the experimental and the calculated cross sections is shown in Figures 2−8.

Analysis of SANS Data. *1. Calculation of the Scattering Intensity.* The coherent differential scattering cross section ($d\Sigma/d\Omega$) derived by Hayter and Penfold[45−48] and Chen[49,50] can be reduced to eq 1 for an assembly of a monodisperse system of micelles

$$d\Sigma/d\Omega = nV_m^2(\rho_m - \rho_s)^2P(Q)S(Q) \quad (1)$$

where n denotes the number density of the micelles or mixed micelles; ρ_m and ρ_s are, respectively, the scattering length densities of the micelles or mixed micelles and the solvent; and V_m is the volume of the micelle. $P(Q)$ is the single (orientationally averaged) particle (intraparticle) structure factor, and $S(Q)$ is the interparticle structure factor. For the analysis, we assume the micelles to be monodisperse prolate ellipsoids ($a = c \neq b$), where the sphere is a special case of that. It may be mentioned, however, that the elongated micelles usually tend to be of varying sizes and may not be monodisperse. In the present analysis, we have assumed the system to be monodisperse to avoid additional unknown parameters. Then, eq 1 can be rewritten as

$$d\Sigma/d\Omega = (c - c_m)V_m^2(\rho_m - \rho_s)^2P(Q)S(Q)/N \quad (2)$$

where $(c - c_m) = nN$; c_m is cmc; and c is the surfactant concentration. The aggregation number N for the micelle is related to the micellar volume V_m by the relation $N = V_m/\upsilon$, where υ is the volume of the individual surfactant molecule.

Now the volume of the mixed micelles may be calculated using eq 3

$$V_m = N(x_A\upsilon_A + x_I\upsilon_I) = (N_A\upsilon_A + N_I\upsilon_I) \quad (3)$$

where υ_A and υ_I are the volumes of surfactant $2A_n$ and surfactant $2I_n$, respectively. $N = (N_A + N_I)$; N_A and N_I are the aggregation numbers of the $2A_n$ and $2I_n$ surfactants in the mixed micelle, respectively.

The scattering length density of mixed micelles is obtained from eq 4

$$\rho_m = (x_A\rho_A + x_I\rho_I) \quad (4)$$

where the ρ_A and ρ_I are the scattering length densities due to $2A_n$ and $2I_n$ surfactants, respectively.

The form factor $P(Q)$ for an ellipsoidal particle is given by eq 5

$$P(Q) = \int [F(Q, \mu)]^2 d\mu \quad (5)$$

where μ is the cosine of the angle between the axis of resolution and Q.

The form factor $F(Q, \mu)$ is given by eq 6, i.e.

$$F(Q, \mu) = 3(\sin w - w\cos w)/w^3 \quad (6)$$

where $w = Q[a^2\mu^2 + b^2(1 - \mu^2)]^{1/2}$ and a and b are, respectively, the semiminor and semimajor axes of the ellipsoid of revolution.

2. Structure Factor for the Interacting Micelles. The interparticle structure factor $S(Q)$ depends on the spatial distribution of micelles. Unlike the calculation of $P(Q)$, it is quite complicated to calculate $S(Q)$ for any other shapes than spherical. This is because $S(Q)$ depends on the shape as well as on the orientation of the particles, and there are no analytical expressions available to calculate it for the asymmetric particles. In the following analysis, we have calculated $S(Q)$ using mean spherical approximation as developed by Hansen and Hayter.[47] The theory is applicable if there is no angular correlation between the particles. This assumption is quite reasonable for charged micelles especially when the surfactant concentration is low and the ratio of the semimajor and semiminor axes is not much greater than unity. Strong electrostatic repulsions prohibit close proximity between two micelles. In the following, the ellipsoidal micelle is approximated by an equivalent sphere of radius $R = (a^2b)^{1/3}$. The intermicellar interaction is modeled via a screened Coulomb potential, and $S(Q)$ is calculated in mean spherical approximation. In the analysis, the only unknown parameters in $d\Sigma/d\Omega$ are the effective monomer charge (α) and the aggregation number (N).

The data in Figures 2 and 3 and 5−8 (corresponding to different micelles and mixed micelles) were first analyzed using eq 2. Then, N, a, and α were taken as the parameter of the fit. The surfactant molecular volume, υ, for the gemini surfactant ($2A_n$ and $2I_n$) was calculated[51,52] using Tanford's formula: $\upsilon = (2\upsilon_1 + \upsilon_2 + 2\upsilon_3)$ Å^3; $2\upsilon_1$ is the volume of two tails with the headgroups; υ_2 is the volume of the spacer chain; and $2\upsilon_3$ is the volume of the two ammonium or imidazolium headgroups, respectively. The scattering length densities for the surfactants were calculated by multiplying each element with the known scattering length densities of each element present in the surfactants. The semimajor axis b ($3n\upsilon/4\pi a^2$) was obtained from the knowledge of the above parameters. The values of N, α, a, and b are given in Tables 2−5. The effects of temperature on micellar sizes were also obtained by similar methods. Most of the fitting data have reduced the chi-square values in the range of 1−5.

Determination of Compositions of the Mixed Micelles. For the calculation of the composition, Clint's theory[53] of assuming an ideal mixing of the surfactant components has been employed, which in turn makes it possible to calculate monomer concentrations and micelle compositions above the cmc of the mixed micellar system under examination. On the basis of this model, the mixed cmc (c^{mix}), unaggregated monomer concentrations (c_{2A} and c_{2I}), and the mole fraction of surfactant $2A_n$ and $2I_n$ in the mixed micelles as a function of the total surfactant concentration are calculated from the cmc's of the pure component and the bulk mole fraction of the components in the surfactant mixture by

$$1/c^{mix} = \tau/c_{2A} + \tau/c_{2I}$$

$$c_{2I} = \{-(c - \Delta_{cmc}) + [(c - \Delta_{cmc})^2 + 4\tau c\Delta_{cmc}]^{1/2}\}/2(c_{2I}/c_{2A} - 1)$$

$$c_{2I} = (1 - c_{2A}/c_{2A}^{cmc})c_{2I}^{cmc}$$

$$x_{2A} = (\tau c - c_{2A})/(c - c_{2I} - c_{2A})$$

$$x_{2A} + x_{2I} = 1$$

dx.doi.org/10.1021/jp304700t | J. Phys. Chem. B 2012, 116, 13239−13247

where τ is the mole fraction of the surfactant; 16-Im (I_0) is the total mixed solute; c_{2A}^{cmc} and c_{2I}^{cmc} are the cmc's of the pure individual surfactants $2A_n$ and $2I_n$; Δ_{cmc} is ($c_{2A}^{cmc} - c_{2I}^{cmc}$); and c is the total surfactant concentration.

RESULTS AND DISCUSSION

The monomeric imidazolium surfactant, I_o (**1**), was obtained upon reaction of *N*-methylimidazole with *n*-hexadecyl bromide in refluxing ethanol for 2 days. *N*,*n*-Hexadecyl imidazole was synthesized by reacting imidazole with *n*-hexadecyl bromide in the presence of K_2CO_3/KI in acetone for 2 days. All the imidazolium gemini surfactants **2a–h** were obtained by refluxing the corresponding α,ω-dibromoalkanes with *N*,*n*-hexadecyl imidazole in dry ethanol at ~80 °C for 48 h as reported earlier.[41] The bis(quaternary ammonium) surfactants **4a–g** (Chart 1) were synthesized as described in the reported procedure.[21]

Variations of the cmc's in Gemini Surfactants. The cmc data for the series of gemini imidazolium surfactants ($2I_n$, $2Br^-$) and that of the gemini ammonium surfactants ($2A_n$, $2Br^-$) including the corresponding monomeric counterparts, I_0 and A_0, have been summarized in Table 1. It shows that the transition from monomeric I_0 to a gemini $2I_n$ molecular architecture has a profound effect on the cmc values, and the dimeric $2I_n$ starts to form micelles at considerably lower concentrations. Figure 1 shows that the cmc values pass through a minimum around n = 3, which again increase with the further increase of the *n*-value and plateau off at higher *n*-value. On the other hand, it is reported in the literature that ammonium-based cationic gemini surfactants have slightly different cmc trends as a function of the spacer lengths.[54,55] Zana and co-workers reported that cmc values for $2A_n$ surfactants go through a maximum at n = 6, and with higher spacer length cmc goes down.[54]

Table 1. Variations of the cmc Values As a Function of the Spacer Length (n) of $2I_n$ and $2A_n$[a] Micellar Systems

surfactant	cmc (10^{-5} M)	surfactant	cmc (10^{-5} M)
A_0	80[42]	I_0	45 ± 0.12
$2A_2$	–	$2I_2$	3.41 ± 0.10
$2A_3$	2.5 ± 0.15	$2I_3$	0.48 ± 0.15
$2A_4$	2.7 ± 0.10	$2I_4$	2.22 ± 0.10
$2A_5$	3.6 ± 0.10	$2I_5$	2.69 ± 0.12
$2A_6$	4.3 ± 0.20	$2I_6$	5.01 ± 0.05
$2A_8$	3.3 ± 0.15	$2I_8$	5.12 ± 0.06
$2A_{10}$	2.7 ± 0.15	$2I_{10}$	6.07 ± 0.05
$2A_{12}$	2.0 ± 0.10	$2I_{12}$	6.19 ± 0.05

[a]The cmc values of $2A_n$ gemini surfactants are taken from our previous report for comparison.[21]

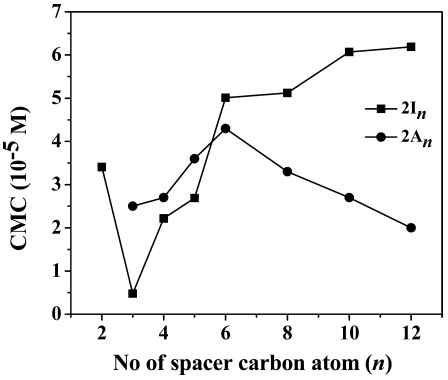

Figure 1. Variation of critical micellar concentrations of $2I_n$ and $2A_n$ surfactants against the number of spacer carbon atoms. The monomeric surfactant, I_0, has been taken here as having spacer n = 0.

Neutron Scattering Studies. In a neutron scattering experiment, a beam of neutrons is directed upon the sample under examination, and the intensities of the neutron scattering in different directions are measured. Since neutrons are scattered by the nuclei in the sample, even isotopes of the same elements can differ in their scattering power. Thus, by taking micellar aggregates in D_2O rather than in H_2O, the scattering densities of various regions can be obtained since deuterons and protons differ widely in their respective scattering capacities. As reported earlier, SANS measurements provide useful information pertaining to the shapes of various self-organizing systems in a noninvasive manner.[16–20] Consequently, we examined how the series of different gemini micelles adopt various morphologies and internal packing arrangements in aqueous media depending on their spacer chain length (n) and nature of cationic headgroup, i.e., ammonium vs imidazolium ions.

Neutron Cross Sections. First, we report the result of the measurements of the neutron cross sections from the micellar solutions of gemini surfactants with ammonium headgroups, $2A_n$, in D_2O as a function of the *n*-values at a fixed surfactant concentration (25 mM). For the sake of comparison, the data for the pure CTAB (A_0) solution (c = 50 mM, a concentration at which CTAB is known to form elongated, nonspherical micelles[56]) are also shown in Figure 2. SANS distributions for

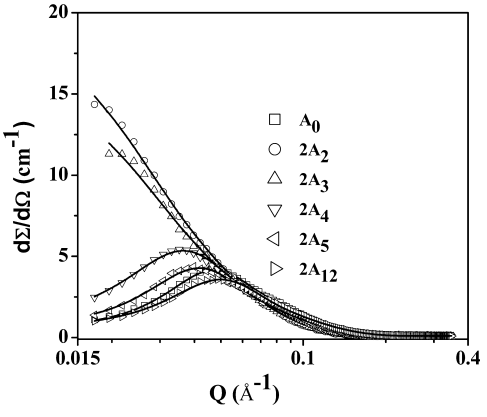

Figure 2. SANS distributions from the micellar systems of CTAB (A_0) and various ammonium gemini surfactants $2A_n$ with different spacer lengths (n = 2, 3, 4, 5, and 12) at 50 °C. The concentration of A_0 was 50 mM, and all the gemini surfactants were taken as 25 mM.

dx.doi.org/10.1021/jp304700t | J. Phys. Chem. B 2012, 116, 13239–13247

Table 2. Effect of the Spacer Length (n) in $2A_n$ Micellar Systems on Q-Value[a,b]

surfactant	spacer length (n)	aggregation number (N)	effective monomer charge (α)	monomer volume (v) (Å^3)	semiminor axis ($a = c$) (Å)	semimajor axis (b) (Å)	b/a
A_0	'0'	115 ± 9	0.18 ± 0.03	555.7	20.1 ± 0.5	37.9 ± 1.1	1.89
$2A_2$	2	353 ± 32	–	1115.5	25.7 ± 0.5	142.4 ± 7.4	5.54
$2A_3$	3	273 ± 25	–	1142.4	23.8 ± 0.5	131.4 ± 6.5	5.52
$2A_4$	4	112 ± 9	0.14 ± 0.02	1169.3	20.0 ± 0.5	78.0 ± 2.4	3.90
$2A_5$	5	79 ± 6	0.23 ± 0.04	1196.2	19.5 ± 0.5	59.5 ± 1.5	3.05
$2A_{12}$	12	44 ± 3	0.33 ± 0.06	1384.5	17.5 ± 0.4	47.8 ± 1.1	2.73

[a]The b/a values of $2A_n$ (n = 2, 3, 4, 5, and 12) are given for comparison with that of the corresponding monomeric surfactant, A_0. [b]All the SANS spectra were taken at 50 °C using 25 mM $2A_n$ micelles. This $2A_n$ molecule may be considered as the dimer of two CTAB monomers linked by a $-(CH_2)_n-$ spacer. For CTAB, n is assumed to be 'zero' (A_0), and the SANS data were collected with 50 mM CTAB.

25 mM of each of $2A_n$, n = 4, 5, and 12, showed well-defined peaks as was the case with pure 50 mM CTAB solution. This peak arises because of a corresponding peak in the interparticle structure factor $S(Q)$.

Usually, this peak occurs at $Q_m = 2\pi/d$, where d is the average distance between the micelles. It is seen that the calculated distributions give the peak positions in $d\Sigma/dQ$ with a good correspondence with the experimentally determined points. Since the Q_m was found to vary with n, one can easily conclude that the number density (n) of micelles is not the same in the above samples even when they have identical surfactant concentration. The micelles derived from gemini surfactant, n = 2 and 3, samples do not show any correlation peak (in this instrument), suggesting that for these dispersions $Q_m < 0.017$ Å^{-1}. When we compared this result at elevated temperature (50 °C) with the reported result at 30 °C,[21] we see the presence of a correlation peak for n = 4; hence, the structural parameter of the resulting micelles can be obtained at the elevated temperature (Table 2). The above observations imply that the aggregation number of the micelles, N, depends on the spacer chain length, n. It is, however, not apparent that the micelles are spherical. Consequently, in the following analysis, we assume them to be prolate ellipsoids ($a = c \neq b$), the sphere being a special case of that.

All the imidazolium gemini surfactants $2I_n$ could be readily dissolved in D_2O, and the resulting samples were optically translucent but remained stable for several weeks without any increase in the optical scatter. The SANS analysis was performed using 25 mM of the gemini $2I_n$ (n = 2, 3, 4, 5, 8, and 12) micelles at 50 °C. The data from the monomeric I_0 micelles at 50 mM are also shown in the same figure (Figure 3).

These data show trends similar to that observed for the $2A_n$ series of gemini surfactants based on the ammonium headgroup. Since the Q_m was found to vary with the number of spacer carbon atoms (n) and type of surfactants, it may be inferred that intermiceller distance and hence the number density of micelles are not the same for different surfactants even at identical surfactant concentrations. Here also, the aggregation number of the micelles, N, was found to depend on the spacer chain length, n (Table 3). Furthermore, it is clear that aggregation number (N) decreased with increasing spacer length akin to that for the $2A_n$ series. However, the changes in aggregation numbers of the imidazole-based micelles were found to be more than that of the ammonium surfactants (Figure 4A). This is presumably due to the planar delocalized nature of the aromatic headgroup and enhanced electrostatic repulsion. Consequently, they would require more space per individual surfactant with increasing spacer length. Hence,

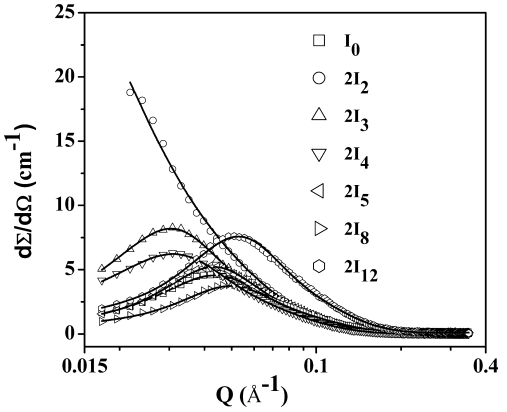

Figure 3. SANS distributions from the micellar systems of I_0 and different imidazolium gemini surfactants $2I_n$ with different spacer lengths (n = 2, 3, 4, 5, 8, and 12) at 50 °C. The concentration of I_0 was 50 mM, and all the gemini surfactants were taken using 25 mM of its concentration.

fewer surfactant molecules may be accommodated into a single micellar aggregate.

Both the semimajor (b) and the semiminor axes (a, c) as well as the axial ratio (b/a) decreased with an increase in the number of spacer carbon atoms (n) (Figure 4 and Tables 2 and 3) for both types of surfactant series. The effective fractional charge (α) on micelles appeared to increase with the increase in n-value (Figure 4 and Tables 2 and 3). Since spheroids and ellipsoids differ in terms of curvature, *larger* effective charge would be expected for a *spheroidal* micelle, and *smaller* effective charge would be indicated for an *ellipsoidal* morphology. This is further substantiated by the changes in the b/a value as a function of n-value. Once again, for the imidazolium gemini surfactant series ($2I_n$), the transition of the *ellipsoidal* to *spheroidal* morphology was found to be more susceptible to changes in the spacer carbon atoms (n) than their ammonium counterparts ($2A_n$).

Figures 5 and 6 show the variation of the neutron cross sections for $2A_4$ and $2I_4$ surfactants at different temperatures. As the temperature was increased, the overall neutron cross-section was found to decrease with the peak position shifting to larger Q value. Table 4 records pertinent information based on the above experiment as a function of temperature. The degree of ionization, which plays an important role for the modification of the magnitude of the electrostatic repulsion at the level of the headgroups, increases with the increase in temperature.[57] This leads to an increase in the headgroup area of the surfactant molecules in the micelles and results in a decrease in the aggregation number, N, for both types of

Table 3. Effect of Spacer Length (n) on $2I_n$ Micellar Systems on Q-Value[a,b]

surfactant	spacer length (n)	aggregation number (N)	effective monomer charge (α)	monomer volume (v) (Å^3)	semiminor axis (a = c) (Å)	semimajor axis (b) (Å)	b/a
I_0	'0'	143 ± 12	0.10 ± 0.02	596.2	20.5 ± 0.5	48.2 ± 1.7	2.35
$2I_2$	2	497 ± 42	–	1191.4	24.7 ± 0.5	233.2 ± 10.3	9.44
$2I_3$	3	189 ± 17	0.12 ± 0.02	1218.3	20.3 ± 0.5	133.4 ± 5.4	6.57
$2I_4$	4	161 ± 14	0.13 ± 0.02	1245.2	20.2 ± 0.5	116.8 ± 4.4	5.78
$2I_5$	5	71 ± 5	0.27 ± 0.05	1272.1	20.0 ± 0.5	54.1 ± 1.1	2.71
$2I_8$	8	46 ± 4	0.34 ± 0.06	1352.8	18.1 ± 0.4	45.4 ± 1.9	2.51
$2I_{12}$	12	37 ± 3	0.37 ± 0.06	1460.4	17.5 ± 0.4	41.8 ± 1.5	2.39

[a]All the SANS spectra were taken at 50 °C using 25 mM $2I_n$ micelles. These $2I_n$ molecules may be considered as the dimer of two C_{16}–Im monomers linked by a $-(CH_2)_n-$ spacer. For C_{16}–Im, n is assumed to be 'zero' (I_0), and the SANS data were collected using 50 mM of its concentration. [b]The b/a values of 2In (n = 2, 3, 4, 5, 8, and 12) are given for comparison with that of the corresponding monomeric surfactant, I_0.

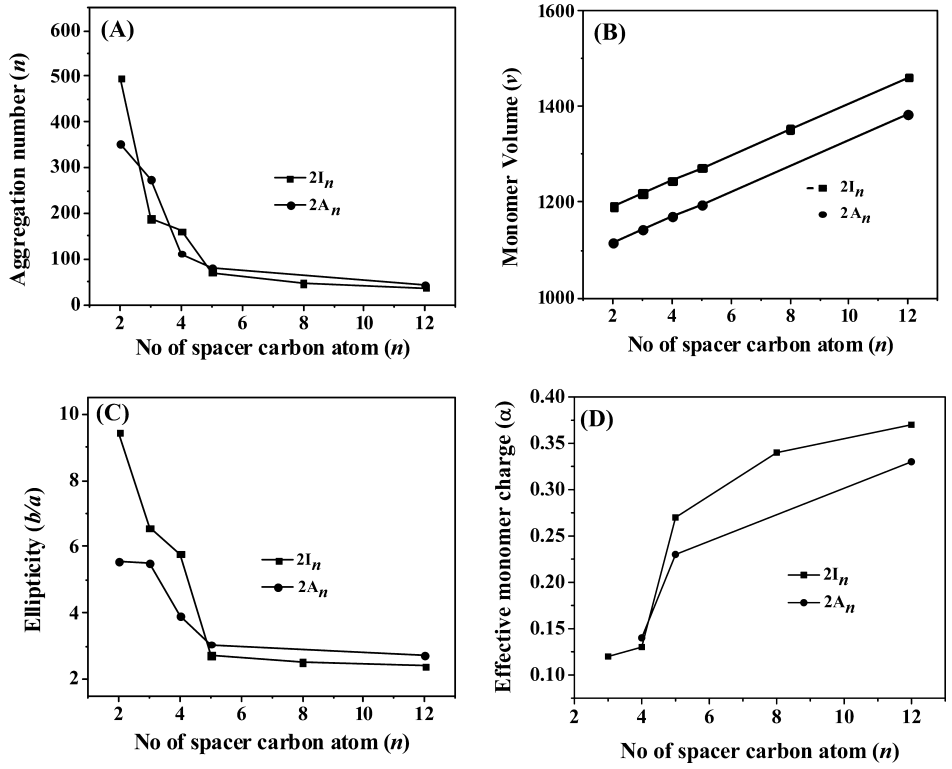

Figure 4. Comparative effect of the spacer carbon atoms (n) for $2I_n$ and $2A_n$ micelles on (A) the aggregation number, (B) the monomer volume, (C) the ellipticity, and (D) the effective monomer charge.

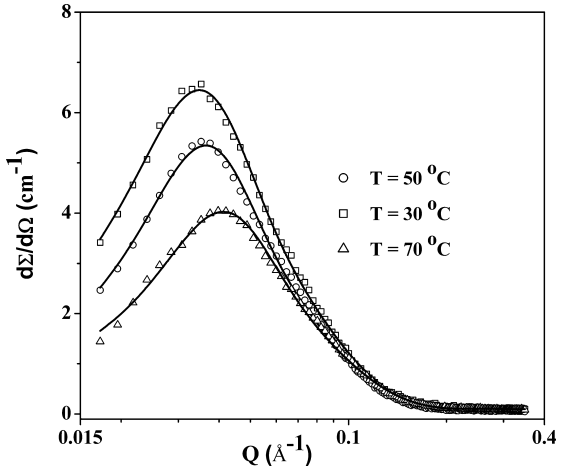

Figure 5. SANS distributions from 25 mM $2A_4$ gemini micelles at various temperatures.

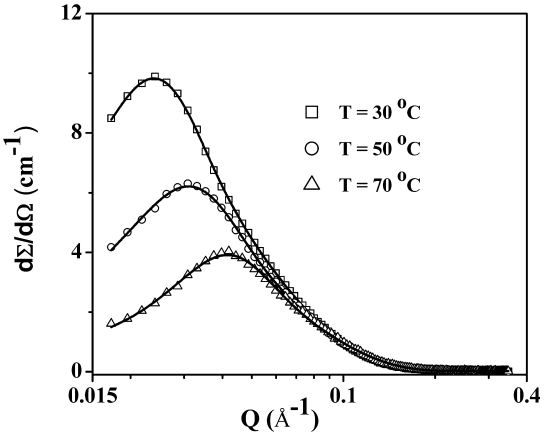

Figure 6. SANS distributions from 25 mM $2I_4$ gemini micelles at various temperatures.

dx.doi.org/10.1021/jp304700t | J. Phys. Chem. B 2012, 116, 13239–13247

Table 4. Effect of Temperature Variation on the *Q*-Value Due to the Micellar $2A_4$ and $2I_4$ Systems at Fixed Concentration of 25 mM

temperature (°C)	aggregation number (N)	effective monomer charge (α)	monomer volume (v) (Å^3)	semiminor axis ($a = c$) (Å)	semimajor axis (b) (Å)	b/a
			(a) 25 mM $2A_4$, $2Br^-$			
30	126 ± 12	0.11 ± 0.02	1169.3	20.6 ± 0.5	82.3 ± 3.8	4.00
50	112 ± 10	0.14 ± 0.03	1169.3	20.0 ± 0.5	78.0 ± 3.1	3.90
70	79 ± 7	0.18 ± 0.03	1169.3	19.4 ± 0.5	58.7 ± 2.0	3.03
			(b) 25 mM $2I_4$, $2Br^-$			
30	398 ± 35	0.09 ± 0.02	1245.2	22.0 ± 0.5	245.5 ± 10.4	11.16
50	161 ± 14	0.13 ± 0.02	1245.2	20.2 ± 0.5	116.8 ± 4.4	5.78
70	76 ± 7	0.19 ± 0.03	1245.2	19.5 ± 0.5	59.8 ± 2.1	3.07

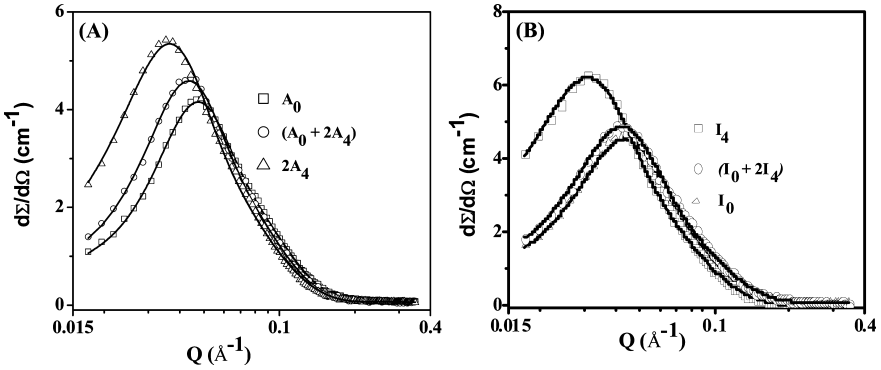

Figure 7. SANS distributions from the mixed micelles of (A) A_0 and gemini surfactants $2A_4$ and (B) I_0 and gemini surfactants at 50 °C. The concentrations of A_0, I_0, $2A_4$, and $2I_4$ were 25, 25, 12.5, and 12.5 mM, respectively.

Table 5. Q-Values Obtained from the SANS Studies of Mixed Micellar Systems[a]

system	aggregation number (N)	effective monomer vcharge (α)	monomer volume (v) (Å^3)	semiminor axis ($a = c$) (Å)	semimajor axis (b) (Å)	b/a
			(a) 25 mM A_0, $2Br^-$ + 12.5 mM $2A_4$, $2Br^-$			
A_0	115 ± 9	0.18 ± 0.03	555.7	20.1 ± 0.5	37.9 ± 1.1	1.89
$2A_4$	112 ± 9	0.14 ± 0.02	1169.3	20.0 ± 0.5	78.0 ± 2.4	3.90
($2A_4$ + A_0)	110 ± 9 (37/73)[b]	0.17 ± 0.03	758.2	20.1 ± 0.5	49.3 ± 1.6	2.45
			(b) 12.5 mM I_0, $2Br^-$ + 12.5 mM $2I_4$, $2Br^-$			
I_0	143 ± 12	0.10 ± 0.02	596.2	20.5 ± 0.5	48.2 ± 1.7	2.35
$2I_4$	161 ± 16	0.13 ± 0.02	1245.2	20.2 ± 0.5	116.8 ± 4.4	5.78
($2I_4$ + I_0)	107 ± 9 (72/35)[b]	0.12 ± 0.02	810.4	20.3 ± 0.5	50.3 ± 1.8	2.48
			(c) 25 mM A_0, $2Br^-$ + 25 mM I_0, $2Br^-$			
A_0	115 ± 9	0.18 ± 0.03	555.7	20.1 ± 0.5	37.9 ± 1.1	1.89
I_0	143 ± 12	0.10 ± 0.02	596.2	20.5 ± 0.5	48.2 ± 1.7	2.35
(A_0 + I_0)	131 ± 11 (66/66)[b]	0.12 ± 0.02	576.0	20.2 ± 0.5	43.9 ± 1.5	2.17
			(d) 12.5 mM $2A_4$, $2Br^-$ + 12.5 mM $2I_4$, $2Br^-$			
$2A_4$	112 ± 9	0.14 ± 0.02	1169.3	20.0 ± 0.5	78.0 ± 2.4	3.90
$2I_4$	161 ± 14	0.13 ± 0.02	1245.2	20.2 ± 0.5	116.8 ± 4.4	5.78
($2A_4$ + $2I_4$)	126 ± 12 (63/63)[b]	0.14 ± 0.02	1207.3	20.0 ± 0.5	91.0 ± 3.4	4.55

[a]All the SANS spectra of mixed micelles were taken at 50 °C. [b]The two values in the parentheses show the aggregation numbers of the individual components in the mixed micelles.

micelles. However, the imidazolium-based surfactant ($2I_4$) was found to be more temperature sensitive, and its N value came down to 76 from 398; the effect was not as pronounced in the case of ammonium-based $2A_4$ micelles (reducing to 79 from 126). Similarly, for both the micelles the effective fractional charge per monomer increased with the increase in temperature. Since a smaller effective charge indicates a more ellipsoidal morphology, increasing temperature appears to induce ellipsoid-to-spheroid transition for micelles derived from both types of gemini surfactants, i.e., $2A_4$ and $2I_4$. This notion is further supported from the concomitant decrease in b/a values upon an increase in temperature. Once again, it is to be noted, however, that $2I_4$ micelles are considerably more temperature sensitive for the ellipsoid-to-spheroid transition than their ammonium counterparts.

Mixed Micellar Systems. Next, we have investigated the structural aspects of the mixed micelles derived from different types of surfactants. Ideal mixing, combined with the pseudophase separation model,[22] is useful for predicting micellar compositions and the amount of nonaggregated surfactant of total surfactant concentration above the cmc. Since the amount of the nonaggregated surfactant and the

dx.doi.org/10.1021/jp304700t | J. Phys. Chem. B 2012, 116, 13239−13247

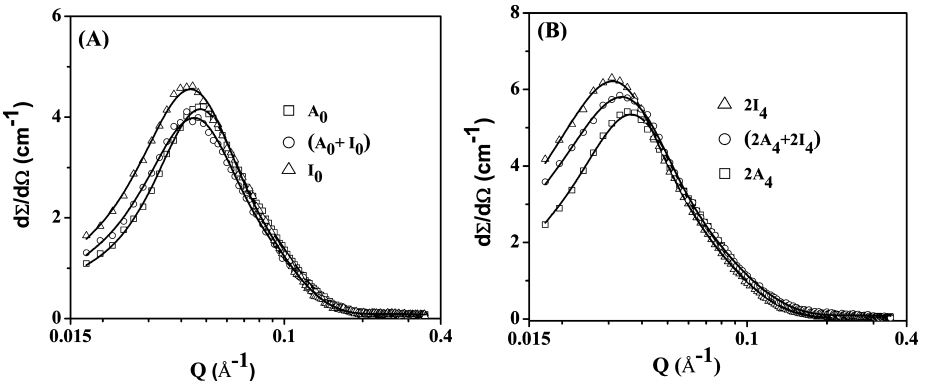

Figure 8. SANS distributions from the mixed micelles of (A) A_0 and I_0 and (B) $2A_4$ and $2I_4$ at 50 °C. The concentrations of A_0, I_0, $2A_4$, and $2I_4$ were 25, 25, 12.5, and 12.5 mM, respectively.

micellar composition have contributions to structure factor and scattering amplitude calculations, we decided to have the following assumptions about the micellar composition and free monomer concentration. As the experimental cmc values for the mixed micellar solution matched well with the theoretical values, we assumed that the surfactants mixed ideally.

The SANS measurements for the mixed miceller solutions of the surfactants $2A_n$ and $2I_n$ were carried out at four different compositions at 50 °C. The different compositions used were (a) 25 mM A_0 + 12.5 mM $2A_4$, (b) 25 mM I_0 + 12.5 mM $2I_4$, (c) 25 mM A_0 + 25 mM I_0, and (d) 12.5 mM $2A_4$ + 12.5 mM $2I_4$. Figure 7 shows the comparison of mixed micelles of 25 mM A_0 + 12.5 mM $2A_4$ and 25 mM I_0 + 12.5 mM $2I_4$ with the corresponding individual micelles. In both the mixed micellar systems, only one peak was observed. This rules out the possibility of the coexistence of different micellar domains in such mixed micellar systems. With the incorporation of gemini surfactant in the monomeric micelles, the position of maximum intensity (Q_m) shifts to a lower Q-value with concomitant increase in the maximum intensity. This is reflected in the equivalent aggregation number of the monomers ($N_m = N(A_0) + 2N(2A_4)$, where the gemini surfactant has been considered to be composed of two monomers), the axial ratio (b/a) of the micelles, and the effective fractional charge (α) on the micelles. All these values were found to be in the average regime of the corresponding individual micelles of A_0, $2A_4$, I_0, and $2I_4$ (Table 5).

Figure 8 shows the comparison of mixed micelles of 25 mM A_0 + 25 mM I_0 and 12.5 mM $2A_4$ + 12.5 mM $2I_4$ with the corresponding individual micelles. It is clear that both the monomeric and dimeric imidazolium-based surfactants (I_0 and $2I_4$) show the position of maximum intensity (Q_m) in a comparatively lower Q-value with concomitant increase in the maximum intensity as compared to their ammonium-based counterparts (A_0 and $2A_4$). The corresponding mixed micelles showed intermediate behavior which is evident from equivalent aggregation number of the monomers, the axial ratio (b/a) of the micelle, and the effective fractional charge (α) on micelles (Table 5).

CONCLUSIONS

Micelle formation from the imidazole-based bis-cationic gemini surfactants with variable spacer length was investigated in detail and compared with the corresponding gemini surfactants with ammonium headgroups. SANS studies show that the micellar morphology changes significantly upon variation in the length of the spacer chains. For both ammonium- and imidazolium-based gemini surfactants, at very short spacer length (n = 2, 3, and 4) the micelles behave quite differently. However, for the micelles derived from geminis with relatively longer spacer chains, the micelles become progressively smaller in size. The imidazolium surfactant micelles in comparison to their corresponding counterparts were found to be more sensitive to spacer length mediated ellipsoid-to-spheroid transitions. Furthermore, temperature-induced ellipsoid-to-spheroid transitions also follow a similar trend. Finally, we show that structurally different kinds of micelles when taken together in various proportions mix uniformly, and the resulting mixed micelles behave like new micellar aggregates with properties that are approximately the average of the individual micelles. Interestingly, it is also possible to tune the shape and the properties of the micelles just by changing the compositions of the individual micelles in it.

AUTHOR INFORMATION

Corresponding Author

*Fax: 91-80-23600529. Tel: 91-80-22932664. E-mail: sb@orgchem.iisc.ernet.in.

Author Contributions

⊥These authors contributed equally to this work.

Notes

The authors declare no competing financial interest.

ACKNOWLEDGMENTS

This work was supported in part by a grant from the UGC-DAE consortium for scientific research. S.B. thanks DST for the J.C. Bose Fellowship.

REFERENCES

(1) Israelachvili, J. N. *Intermolecular and Surface Forces*, 2nd ed.; Academic Press: London, 1991.

(2) Israelachvili, J. N. *Physics of Amphiphiles: Micelles, Vesicles and Macroemulsions*; Elsevier: Amsterdam, 1985; p 24.

(3) Wennerstrom, H.; Lindman, B. *Phys. Rep.* **1979**, *52*, 1−86.

(4) Menger, F. M. *Angew. Chem., Int. Ed. Engl.* **1991**, *30*, 1086−1099.

(5) Bhattacharya, S.; Samanta, S. K. *J. Phys. Chem. Lett.* **2011**, *2*, 914−920.

(6) Cutler, W. G.; Vissa, E. *Detergency: Theory and Technology*; Marcel Dekker: New York, 1987.

(7) Dobius, B. In *Phenomena in Mixed Surfactant Systems*; Scamehorn, J. F., Ed.; ACS Symp. Ser., American Chemical Society: Washington, DC, 1986; Vol. *311*, p 216.

(8) Bhattacharya, S.; Kumar, V. P. *Langmuir* **2005**, *21*, 71−78.

(9) Bhattacharya, S.; Kumar, V. P. *J. Org. Chem.* **2004**, *69*, 559−562.
(10) Karaborni, S.; Esselink, K.; Hilbers, P. A. J.; Smit, B.; Karthauser, J.; van Os, N. M.; Zana, R. *Science* **1994**, *266*, 254−256.
(11) Bhattacharya, S.; Snehalatha, K. *Langmuir* **1995**, *11*, 4653−4660.
(12) Manohar, C.; Rao, U. R. K.; Valaulikar, B. S.; Iyer, I. M. *J. Chem. Soc., Chem. Commun.* **1986**, 379−381.
(13) Shikata, T.; Hirata, H.; Kotaka, T. *Langmuir* **1989**, *5*, 398−405.
(14) Haldar, J.; Aswal, V. K.; Goyal, P. S.; Bhattacharya, S. *Angew. Chem., Int. Ed.* **2001**, *40*, 1228−1232.
(15) Bhattacharya, S.; De, S. *Langmuir* **1999**, *15*, 3400−3410.
(16) Berr, S. S.; Jones, R. R. M.; Johnson, J. S. *J. Phys. Chem.* **1992**, *96*, 5611−5614.
(17) Pilsl, H.; Hoffmann, H.; Hoffmann, S.; Kalus, J.; Kencono, A. W.; Lindner, P.; Ulbricht, W. *J. Phys. Chem.* **1993**, *97*, 2745−2754.
(18) Kaler, E. W.; Billman, J. F.; Fulton, J. L.; Smith, R. D. *J. Phys. Chem.* **1991**, *95*, 458−462.
(19) Aswal, V. K.; De, S.; Bhattacharya, S.; Heenan, R. K. *Phys. Rev. E* **1998**, *57*, 776−783.
(20) Zaccai, G.; Blasie, J. K.; Schoenborn, B. P. *Proc. Natl. Acad. Sci. U.S.A.* **1975**, *72*, 376−380.
(21) De, S.; Aswal, V. K.; Goyal, P. S.; Bhattacharya, S. *J. Phys. Chem.* **1996**, *100*, 11664−11671.
(22) De, S.; Aswal, V. K.; Goyal, P. S.; Bhattacharya, S. *J. Phys. Chem. B* **1997**, *101*, 5639−5645.
(23) De, S.; Aswal, V. K.; Goyal, P. S.; Bhattacharya, S. *J. Phys. Chem. B* **1998**, *102*, 6152−6160.
(24) De, S.; Aswal, V. K.; Goyal, P. S.; Bhattacharya, S. *Chem. Phys. Lett.* **1999**, *303*, 295−303.
(25) Haldar, J.; Aswal, V. K.; Goyal, P. S.; Bhattacharya, S. *J. Phys. Chem. B* **2001**, *105*, 12803−12808.
(26) Haldar, J.; Aswal, V. K.; Goyal, P. S.; Bhattacharya, S. *J. Phys. Chem. B* **2004**, *108*, 11406−11411.
(27) Bhattacharya, S.; Haldar, J. *Langmuir* **2004**, *20*, 7940−7947.
(28) Welton, T. *Chem. Rev.* **1999**, *99*, 2071−2084.
(29) Wasserscheid, P.; Keim, W. *Angew. Chem., Int. Ed.* **2000**, *39*, 3772−3789.
(30) Sheldon, R. *Chem. Commun.* **2001**, 2399−2407.
(31) Carmichael, A. J.; Seddon, K. R. *J. Phys. Org. Chem.* **2000**, *13*, 591−595.
(32) Remsing, R. C.; Hernandez, G.; Swatloski, R. P.; Massefski, W. W.; Rogers, R. D.; Moyna, G. *J. Phys. Chem. B* **2008**, *112*, 11071−11078.
(33) Smiglak, M.; Metlen, A.; Rogers, R. D. *Acc. Chem. Res.* **2007**, *40*, 1182−1192.
(34) Liu, G.; Gu, D.; Liu, H.; Ding, W.; Li, Z. *J. Colloid Interface Sci.* **2011**, *358*, 521−526.
(35) Bhadani, A.; Kataria, H.; Singh, S. *J. Colloid Interface Sci.* **2011**, *361*, 33−41.
(36) Ao, M.; Xu, G.; Zhu, Y.; Bai, Y. *J. Colloid Interface Sci.* **2008**, *326*, 490−495.
(37) Dujat, L. C.; Rodrigues, M.; Yagüe, A.; Calpena, A. C.; Amabilino, D. B.; Linares, J. G.; Borràs, M.; García, L. P. *Langmuir* **2012**, *28*, 2368−2381.
(38) Andre, L.; Klaus, L.; Rivo, H. R.; Laurent, W. *Colloid Polym. Sci.* **2005**, *283*, 469−479.
(39) Ao, M.; Huang, P.; Xu, G.; Yang, X.; Wang, Y. *Colloid Polym. Sci.* **2009**, *287*, 395−402.
(40) Bhadani, A.; Singh, S. *Langmuir* **2011**, *27*, 14033−14044.
(41) Dupont, J.; Consorti, C. S.; Suarez, P. A. Z.; de Souza, R. F. *Org. Synth.* **2002**, *79*, 236−241.
(42) Kalyanasundaram, K.; Thomas, J. K. *J. Am. Chem. Soc.* **1977**, *99*, 2039−2044.
(43) Ray, G. B.; Chakraborty, I.; Moulik, S. P. *J. Colloid Interface Sci.* **2006**, *294*, 248−254.
(44) Aswal, V. K.; Goyal, P. S. *Curr. Sci.* **2000**, *79*, 947−953.
(45) Hayter, J. B.; Penfold, J. *J. Colloid. Polym. Sci.* **1983**, *261*, 1022−1030.
(46) Hayter, J. B.; Penfold, J. *J. Mol. Phys.* **1981**, *42*, 109−118.
(47) Hansen, J.-P.; Hayter, J. B. *Mol. Phys.* **1982**, *46*, 651−656.
(48) Hayter, J. B.; Penfold, J. *J. Chem. Soc., Faraday Trans. 1* **1981**, *77*, 1851−1863.
(49) Chen, S. H. *Annu. Rev. Phys. Chem.* **1986**, *37*, 351−399.
(50) Chen, S. H.; Lin, T. L. *Methods of Experimental Physics*; Academic Press: New York, 1987; Vol. *23B*, pp 489−543.
(51) Tanford, C. *J. Phys. Chem.* **1972**, *76*, 3020−3024.
(52) Mortensen, K. *J. Phys.: Condens. Matter* **1996**, *8*, A103−A124.
(53) Clint, J *J. Chem. Soc.* **1975**, *71*, 1327−1334.
(54) Zana, R. *J. Colloid Polym. Sci.* **1980**, *78*, 330−337.
(55) Frindi, M.; Michels, B.; Levy, H.; Zana, R. *Langmuir* **1994**, *10*, 1140−1145.
(56) Danino, D.; Talmon, Y.; Zana, R. *Langmuir* **1995**, *11*, 1448−1456.
(57) Menger, F. M.; Littau, C. A. *J. Am. Chem. Soc.* **1991**, *113*, 1451−1452.